COMPARISON OF THE TECHNICAL PERFORMANCE OF A DISCRETELY SUPPORTED SLAB TRACK SYSTEM AND AN EMBEDDED SLAB TRACK SYSTEM IN A HIGH-SPEED RAILWAY

M. Alkhateeb, (alkhatm2@lsbu.ac.uk), A. Ali (alia76@lsbu.ac.uk), M. Mavroulidou (mavroum@lsbu.ac.uk), M. Gunn (mike.gunn@lsbu.ac.uk), M. Wehbi* (mohamed.wehbi@networkrail.co.uk)

Division of Civil and Building Services Engineering, School of the Built Environment and Architecture, London South Bank University, London, UK, *Network Rail, Birmingham, UK

KEYWORDS: High-Speed Railway, Slab Track, Continuous Support, Discrete Support, Structural Analysis, Rheda Slab Track, Embedded Slab Track

ABSTRACT

Slab tracks are increasingly used for High-Speed Railways (HSR) as opposed to the conventional ballasted track. This is due to many factors, including increased durability and sustainability, as the slab track can sustain higher dynamic loading with less maintenance and disruption to railway services. In line with this, this paper reports on preliminary work on the development and application of a 3D structural model using the Finite Element Analysis (FEA) software ABAQUS. The research aims at evaluating comparatively the behaviour of two types of slab track systems; namely, the RHEDA Track System (RTS), which is a German system, and the Balfour Beatty (UK) Embedded Rail System (ERS). The modelled track structures consist of a rail fastened onto a slab laid on a suitable foundation. The foundation comprises a Hydraulically Bound Layer (HBL) placed on a Frost Protection Layer (FPL) overlaying the subgrade soil. The paper reports on findings of static loading on a straight railway section investigating the relationship between slab the thickness values and the corresponding displacements (deflections) and related stresses along the load path. Ongoing research is further developing the model to assess the dynamic behaviour of HSR slab track including the railway geometry-structure interaction particularly at bends.

1. INTRODUCTION

Recent technological advances led to the rapid development of high-speed railways in the last two decades with many high-speed rail lines planned for the future. This trend is due to the fact that rail travel especially HSR is more environmentally friendly than the road and air mode of transport as the HSR runs on electricity and produces less air pollution. Furthermore, it takes the pressure out of the road network due to fewer cars and therefore lowers traffic congestion. The development of Slab Track (ST) systems allows trains to travel at higher speeds with less maintenance requirements, due to an increased lateral and longitudinal stability. This reduces track closures and consequently allows for higher train frequency (Esveld, 2010).

There have been several finite element models developed for the purpose of optimizing the design of the railway track, especially the ballasted solution for which a number of nonlinear three-dimensional models have been developed (Texeira, 2003). However, compared to traditional ballasted railway tracks, the structure and mechanics of embedded rail track systems are different and merit further targeted research currently lacking (Liu et al. 2011): at present the majority of studies on ballastless track analyses conducted focused on the dynamic behaviour and wave propagation and direct effects on slab track design with respect to vertical loads that act on the ST but only few works considered the dynamic

loads that occur on the high-speed ST structure, i.e. moving point loads (causing excess vibration at critical velocity, hence ST deterioration), moving dynamic loads (occurring when wheel/rail profile is asymmetrical, causing wheel deterioration) and fixed point dynamic loads (produced when the wheel passes over irregularities in the ST structure) (Lei, 2016).

This preliminary study is part of ongoing research aimed at addressing this knowledge gap. Examples of previous numerical studies of ballastless systems include amongst other: (a) Markine *et al* (2000) developed a design procedure which includes numerical modelling and dynamic analysis together with laboratory testing and optimisation. They applied the procedure for the design optimization of slab tracks with embedded rails (i.e. ERS) using the model "Rail" developed at Delft University and commercial software ANSYS for 2-D and 3-D finite element models incorporating the track and a moving load. For the design optimisation (based on a numerical optimisation technique) several criteria were considered namely wear and tear of wheels, noise from moving trains and strength of materials and varied component dimensions and track model mechanical properties were used; (b) Fang *et al* (2011), who performed comparative FE study using ABAQUS software of the dynamic responses of three ballastless railway system substructures namely the Japanese ballastless concrete slab track (Slab Track), and two other systems (RACS-1 and RACS-2) with a hot mix asphalt (HMA) layer at different positions in the substructures.

The horizontal stresses, vertical deformation, and acceleration results were analysed. These showed that although the dynamic responses of RACS-1 were similar with Slab Track, HMA layer positively affected the stress distributions and enabled vertical deformation recovery. It was thus concluded that HMA used for railway substructure can enhance resilience, improve the stress distribution, weaken dynamic loading, and lower vibration; (c) Aggestam *et al* (2018) focusing on modelling vehicle–track interaction modelled with a complex-valued modal superposition technique for the linear, time-invariant 2-D track model track and an extended state-space vector approach. The vertical dynamic response can then be calculated by considering a generic initial-value problem initially developed for a ballasted track.

Two generic slab track models including one or two layers of concrete slabs modelled using Rayleigh–Timoshenko beam theory are evaluated and compared to a traditional ballasted track for two application examples involving: (i) the periodic response due to the rail seat passing frequency as influenced by the vehicle speed and a foundation stiffness gradient and (ii) the transient response due to a local rail irregularity (dipped welded joint). The results showed that the studied foundation stiffness gradients had a negligible effect on the wheel–rail contact force for speeds v > 200 km/h however it affected other dynamic responses such as the bending moment in the slab and the load distribution on the foundation were affected. Moreover, a geometrical rail imperfection had a large impact on the wheel–rail contact forces as well as on the bending moment in the panels. Overall, significant dynamic effects were observed in the described examples.

Concerning modelling and design theories of high-speed railway ballastless tracks a review can be found in Liu et al (2011); this review encompasses the calculation methods and parameters concerning train load, thermal effects, and foundation deformation of high-speed railway ballastless track together with the structural design methods. This paper presents the numerical modelling of two different types of ballastless track system, which investigates their comparative behaviour under static loading (17 Ton Axle load), as a first step towards subsequent dynamic loading analysis.

The two systems studied are (a) the German Rheda 2000 system, a widely used discretely supported system, where the rail is supported by sleepers encased in a concrete bearing layer (CBL) and (b) a continuously supported Embedded Rail Structure (ERS), where the rails are embedded into the concrete slab; this offers continuous support so that wheels do not experience any differences in vertical stiffness, a major source of corrugation development (Esveld, 2003). There are various versions of ERS system designs as these have been used in Europe since the 1970s (Tayabji, and Bilow 2001). This paper studies the Balfour Beatty ERS (BB ERS), an innovative low noise ST specifically designed for high speed-rail but also ideal for heavy haul, mixed traffic, metros and light rail. In the BB ERS a block rail (applied to

achieve improved acoustic properties and low structure height, together with pad and shell and this assembly is then grouted into the concrete (see Figure 1).

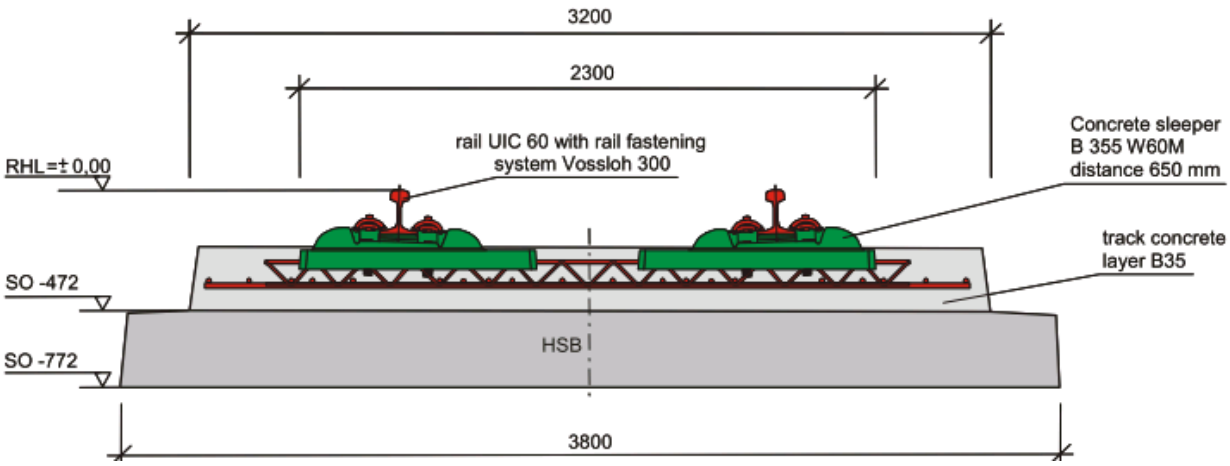

(a)

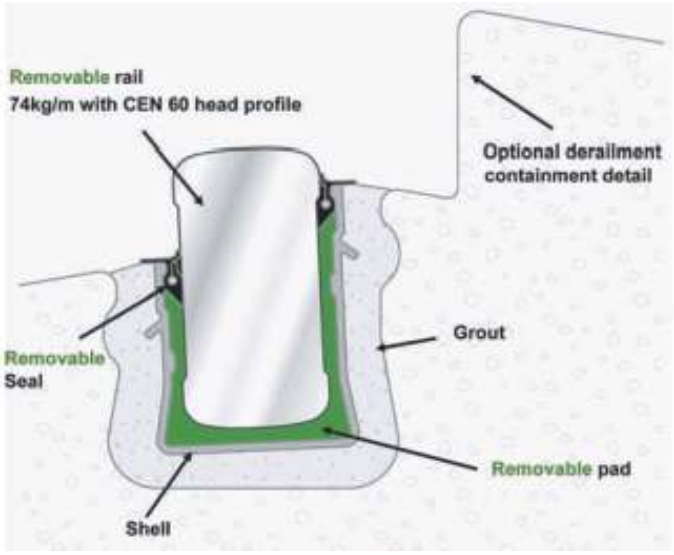

(b)

Figure 1: Typical sections of non-ballasted systems used in this study (a) Rheda 2000; (b) BB ERS (source: Esveld, 2003)

The following sections present the Finite Element model development of these systems in ABAQUS software, and preliminary analysis results for static load conditions.

2. NUMERICAL ANALYSES

2.1. Geometry, Boundary Conditions and Material Properties

Figures 2 represents schematically the 3D model geometry of the RTS whilst the ERS is represented in Figures 3, 4a, 4b and 5. The two systems and the respective Finite Element discretisation use 20-noded quadratic brick elements with reduced integration (C3D20R). The geometry and number of elements for each component is tabulated in Table 1. Note that Table 1 shows five different thicknesses of the CBL (concrete slab) as a parametric study to investigate the effect of the CBL thickness on the displacements

and stress distributions. Table 1 also shows the material properties for the two systems, based on a synthesis of data found in the literature (Batchelor, 1981; Feng, 2011; Michas, 2012). For the subgrade soil, a preliminary parametric study was performed with three different cross section dimensions to represent the theoretical semi-infinite, elastic half space i.e. a 6m x 6m, 8m x 8m and 16m x 16m section respectively.

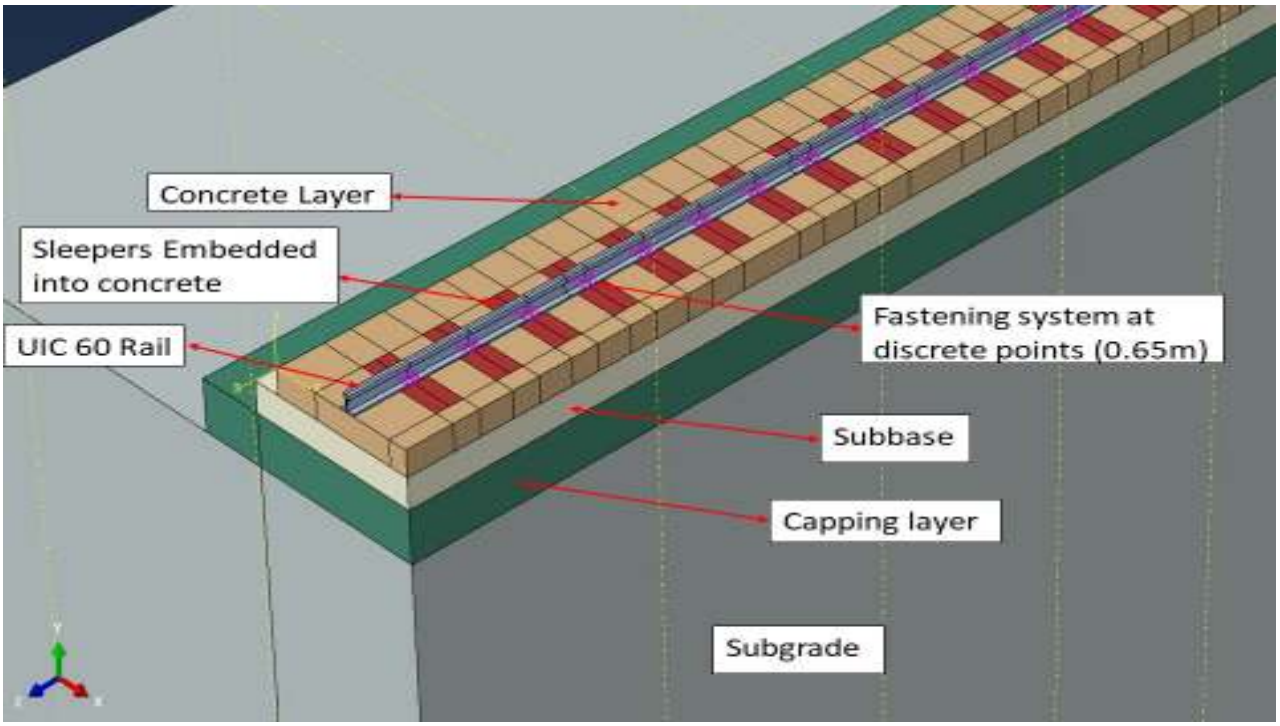

Figure 2. RTS 3D model geometry (ABAQUS)

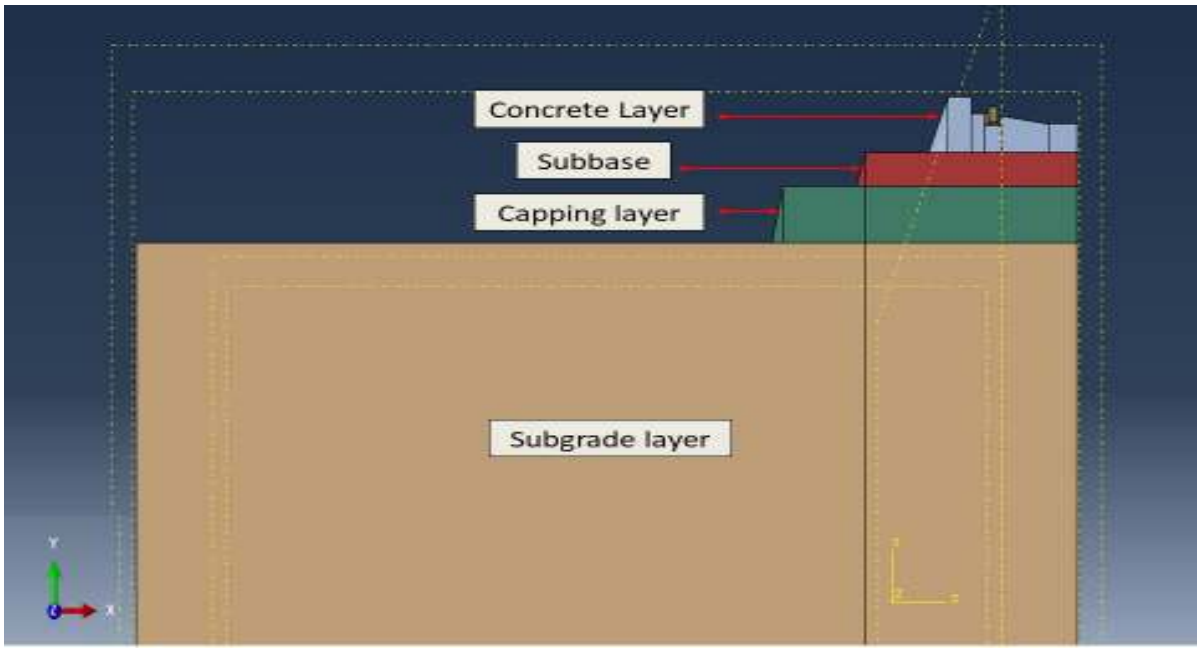

Figure 3. BB ERS 3D model geometry (ABAQUS)

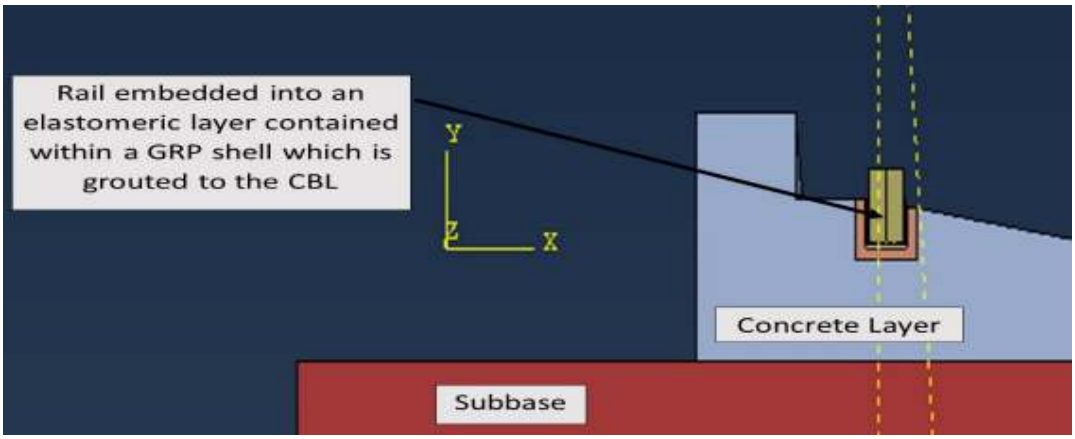

Figure 4a. Section view of BB ERS system

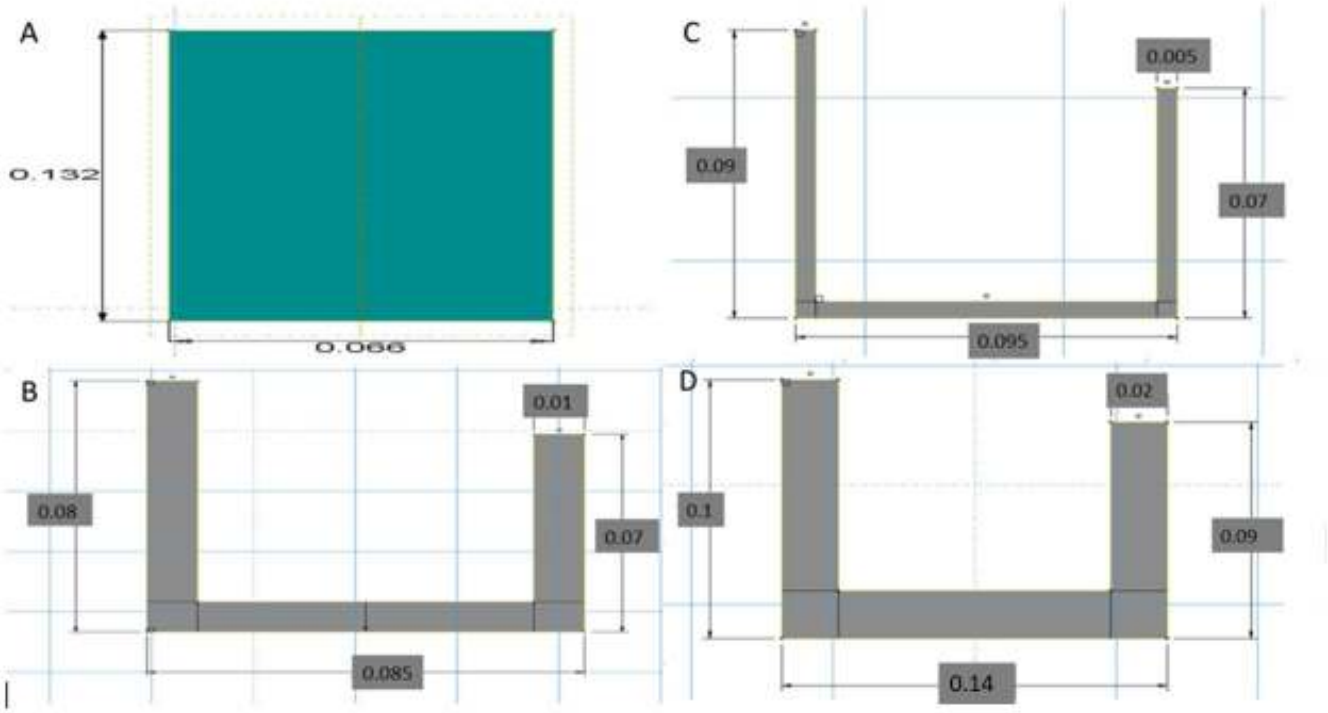

Figure 4b. Embedded components (dimensions (m) are confidential and are approximated), (A) Rectangular rail, (B) Elastomeric pad, (C) GRP shell, (D) Grout

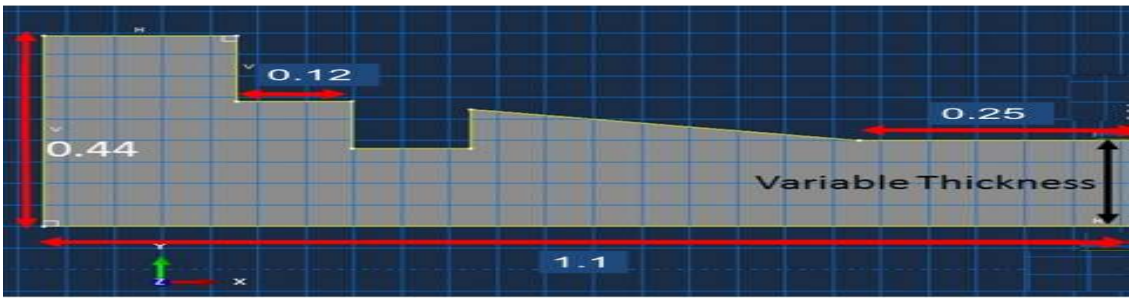

*Only half the cross section was used with a width of 1.1m

Figure 5. BB ERS concrete layer (dimensions (m) are confidential and are approximated)

Table 1. Dimensions and material properties of track layers (quarter symmetry)

System	Track component	Dimensions (m^3)	Number of elements (FE mesh)	Modulus of Elasticity, E (GPa)	Poisson's Ratio, ν
RHEDA2000	**Rail**	UIC60 approx.	990	207	0.28
	Sleeper Concrete	0.914 x 0.12 x 0.29	3120	70	0.2
	CBL (concrete)	1.6 x 0.200 x 21.45	15591	34	0.2
		1.6 x 0.225 x 21.45	15591		
		1.6 x 0.250 x 21.45	21828		
		1.6 x 0.275 x 21.45	21828		
		1.6 x 0.300 x 22.45	21828		
	HBL (Subbase)	1.9 x 0.3 x 21.45	172	5	0.2
	FPL (Capping)	2.6 x 0.5 x 21.45	215	0.12	0.2
	Subgrade soil	8 x 16 x 21.45	22016	0.01	0.4
Balfour Beatty ESR	**Rail**	See Figure 4b	216	207	0.28
	Elastomeric pad		642	61	0.3
	GRP shell		535	17	0.22
	Grout		535	39	0.45
	Concrete Slab	See Figure 5 (The element numbers in the next column correspond to 0.2,0.225,0.25, 0.275 and 0.3m thickness respectively for a slab length of 21.45 m)	15444	70	0.2
			18304		
			19734		
			19734		
			22594		
	HBL (Subbase)	1.9 x 0.3 x 21.45	172	5	0.2
	FPL (capping)	2.6 x 0.5 x 21.45	215	0.12	0.2
	Subgrade soil	8 x 16 x 21.45	22016	0.01	0.4

*in a linear elastic static analysis, the material densities/unit weights do not affect the results

To simulate the loading pattern of a standard two-coach passenger train, a point load of 83.3 kN is applied at eight points (see Figure 6a). Figure 6a also depicts the position of wheels of an approximated standard UIC railway passenger wagon.

The centre to centre distance between the wheels of same bogie is 2.6m whilst the centre to centre distance between two bogies is 3.6m (as derived from the UIC code). Other boundary conditions, which can be seen on the Finite Element meshes shown in Figures 2 and 3, are as described below.

Y-symmetric roller boundary is applied to all the soil vertical boundaries and vertical boundaries parallel to XY plane of all other layers (including rails). This means that nodes in these vertical planes are constrained to remain in the same plane throughout the analysis. The bottom plane of the model is fixed i.e. no translation is allowed in any of the three co-ordinate directions. At the bottom we consider that the underlying material is bedrock (i.e. a much stiffer material) which undergoes no deformations.

Note that the boundary conditions applied to both the models, i.e. ERS and RTS are the same.

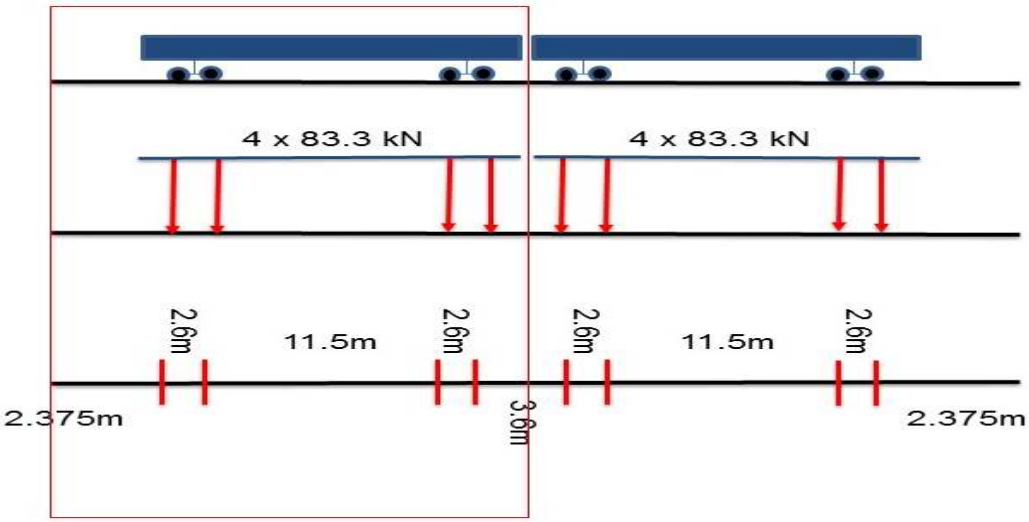

Figure 6a. Loading conditions for the models presented in this paper with the modelled half of track outlined

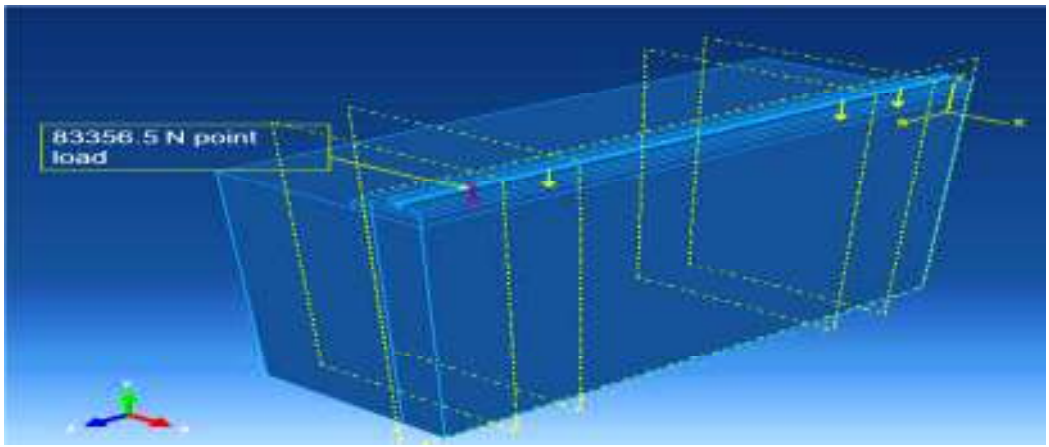

Figure 6b. ABAQUS snapshot of point load positions

2.2 Numerical Results and Discussion

The results of ten finite element analyses are presented in Table 1 and discussed in this section. For each of the ERS and RTS systems we carried out analyses for five different CBL thicknesses (t_e=200mm, t_e =225mm, t_e =250mm, t_e =275mm, and t_e =300mm). In the following we present results for vertical displacement (U2) and vertical stress (S22) as the most significant results although (of course) results for two other displacement components and five other stress components are available.

Figure 7 shows the vertical displacement contours for the RTS and ERS track bed systems; blue means maximum deformation and red means least deformation. The maximum load intensity is situated near the area where the colour of the plot is blue.

Consider Figures 7 and 8, ABAQUS automatically allocates colours to displacement values in these plots. Thus the deep blue colour represents different (although not significantly different) maximum displacements. None-the-less the contour plots demonstrate the essential similarity of the response of the two systems although the structural details of how the rails are supported are quite different. In fact this is the type of response which can be expected on general principles.

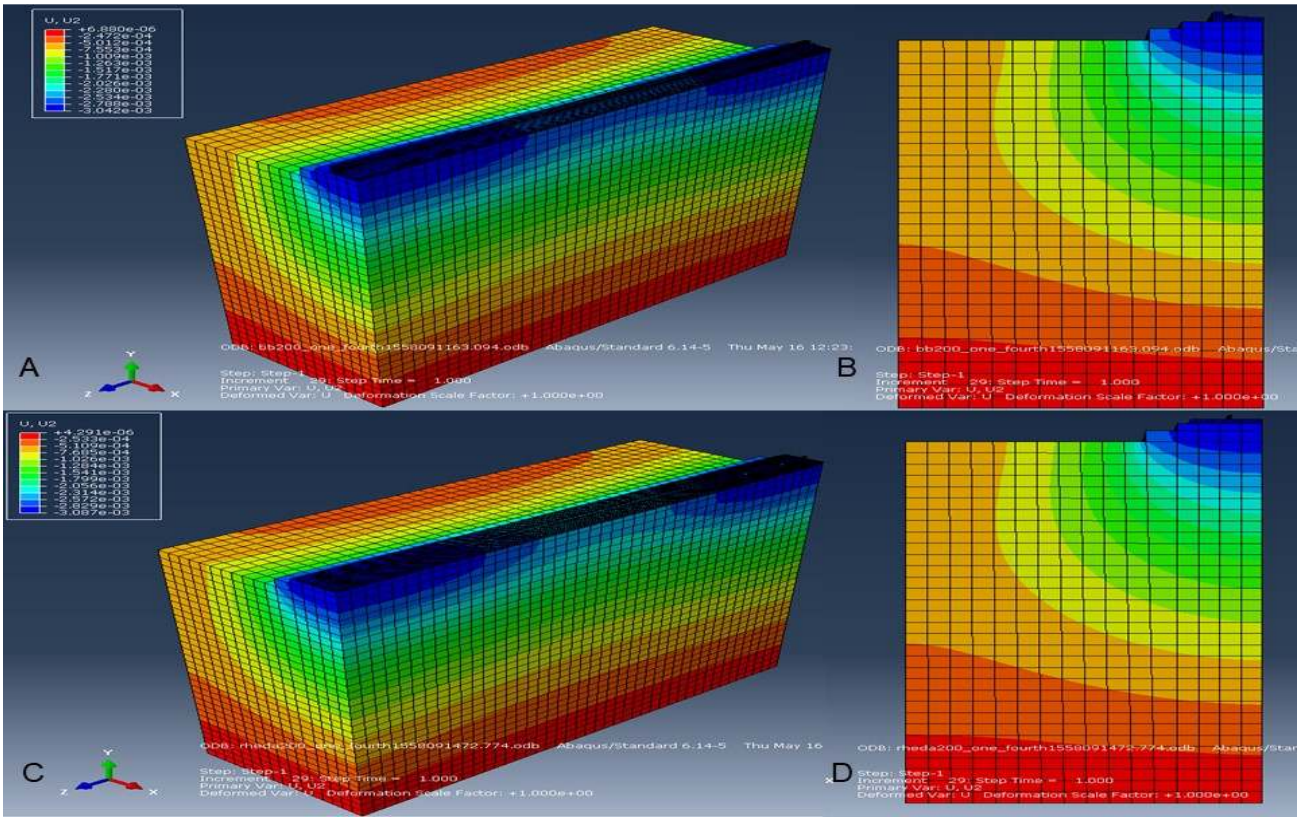

Figure 7. Displacement contours (A) ERS, (B) ERS section view midpoint, (C) RTS, (D) RTS section view midpoint

Figure 8. Displacement values for contour plots, (A) ERS, (B) RTS

The major part of the vertical displacements is a direct result of the compression of the most flexible part of the system (the underlying soil) and the loads applied to both systems are identical. According to Saint-Venant's principle the overall results (particularly some distance from where the loads are applied) will be almost independent of the way the loads are transmitted to the rest of the system by the details of the rail support (i.e. slab track system).

The effects of the variation in the thickness of the main concrete slab on the maximum displacement at the bottom of the slab and on the maximum displacement at the top of the subgrade are shown in Table 2 and Figure 9. Generally, the two systems seem to produce comparatively similar values of displacement.

Table 2. Displacements for the RTS and the ERS at the bottom of the CBL (concrete slab) and at the top of the subgrade soil

	Quarter models (finely meshed)			
Slab Thickness (mm)	Maximum displacement in RTS (m)		Maximum displacement in ERS (m)	
	@ Bottom of concrete slab	@Top of Subgrade	@ Bottom of concrete slab	@Top of Subgrade
200	0.003120	0.003001	0.003024	0.002999
225	0.002997	0.002969	0.002998	0.002974
250	0.002967	0.002941	0.002976	0.002953
275	0.002943	0.002917	0.002959	0.002936
300	0.002921	0.002897	0.002943	0.002921

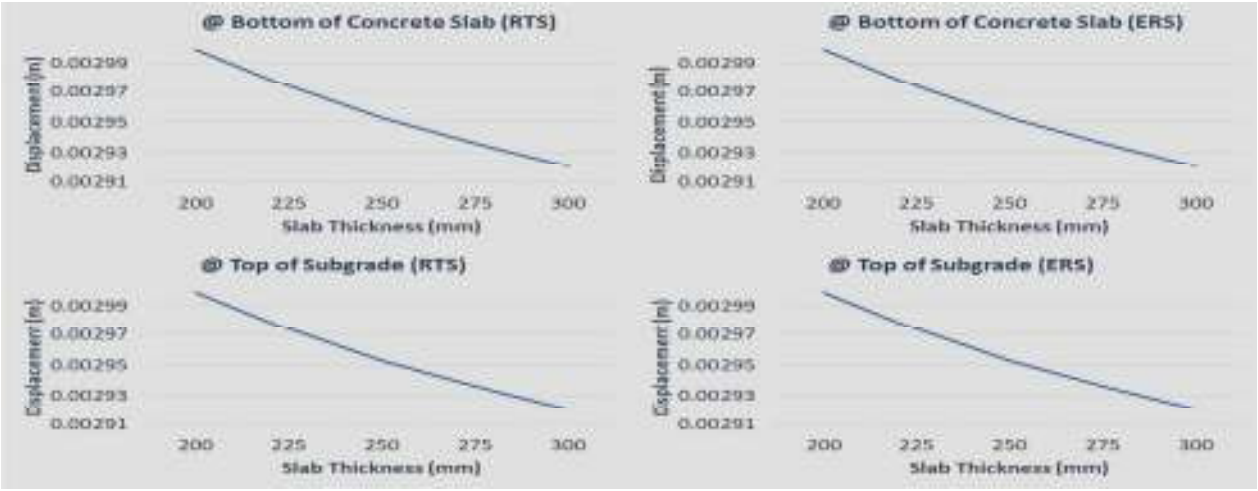

Figure 9. Comparison of thickness versus vertical displacement for RTS and ERS

The effects of the variation in the thickness of the main concrete slab on the maximum stress at the bottom of the slab and on the maximum stress at the top of the subgrade are shown in Table 3 and Figure 10. The results show that whilst the stress at the top of the subgrade is comparable between the two systems, the maximum stress at the bottom of the concrete slab of the RTS is higher than that of the ERS.

Table 3. Maximum stresses for the RTS and the ERS at the bottom of the CBL (concrete slab) and at the top of the subgrade soil

	Quarter models (finely meshed)			
Slab Thickness (mm)	Maximum stress in RTS (Pa)		Maximum stress in ERS (Pa)	
	@ Bottom of concrete slab	@Top of Subgrade	@ Bottom of concrete slab	@Top of Subgrade
200	77314.690	5993.780	50107.650	5977.494
225	63365.880	5794.109	44223.120	5936.263
250	61112.030	5624.439	38065.590	5893.823
275	51103.910	5545.544	32299.300	5868.266
300	43332.440	5500.062	28575.850	5825.750

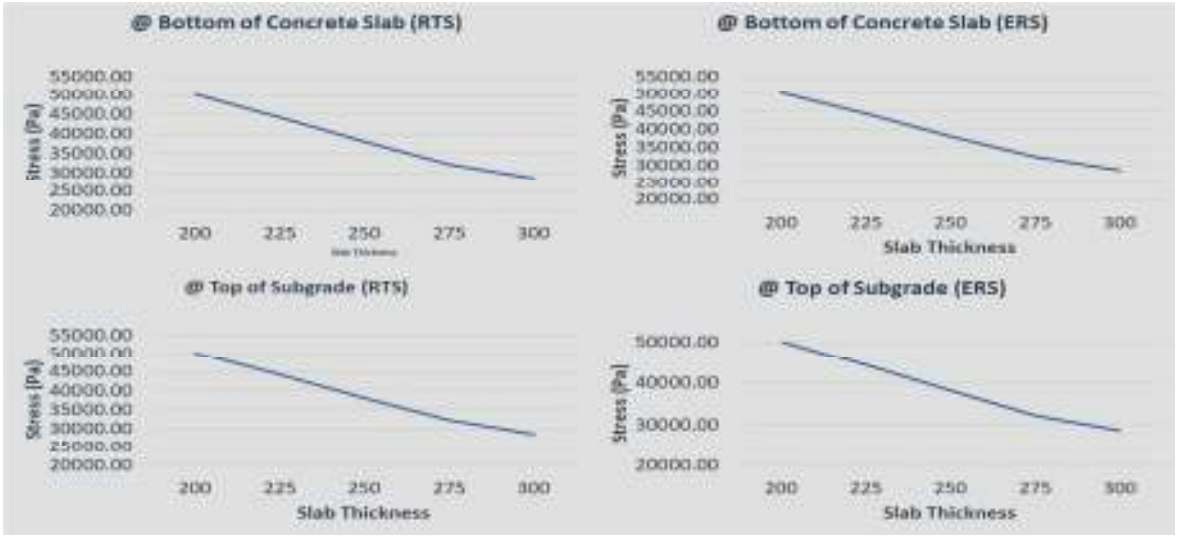

Figure 10. Comparison of thickness versus vertical stress for ERS and RTS

The adjusted values of R-square of the RTS and the ERS for the maximum displacement and maximum stresses at the bottom of the concrete slab and at the top of the subgrade are shown in Table 4. The R values of the ERS system are similar whilst the corresponding R values of the RTS are less similar.

Table 4. Adjusted R-squared values for the linear fit of thickness versus stress and displacement

	RTS		ERS	
Location	@ Bottom of concrete slab	@Top of Subgrade	@ Bottom of concrete slab	@Top of Subgrade
Stress	0.956	0.905	0.991	0. 993
Displacement	0.781	0.989	0.985	0.985

3. CONCLUSIONS

The paper reports the development of two FEA models using Abaqus to investigate the behaviour of track structure of the RTS and the ERS under static loading. The research is part of an on-going project by the authors at London South Bank University (LSBU) to investigate the interaction between the geometrical design and structural design of HSR including dynamic loading at bends.

The main conclusions so far concerning the comparison of the two HSR systems are as follows.

Generally, the two systems appear to produce comparatively similar values of displacement (deflection) at the bottom of the slab and on the maximum displacement at the top of the subgrade.

However, whilst the maximum stress at the top of the subgrade is comparable between the two systems, the maximum stress at the bottom of the concrete slab of the RTS is higher than that of the ERS.

As a complete linear relationship between stress and displacement with the changing thickness of the concrete layer was not established, regression modelling is done on the data and adjusted R-squared values for linear fit for the data in Table 2 and 3 are shown in Table 4.

R-squared value is an indicator of quality of fit. If the R-squared value is equal to 1 then the data will fit a linear model without any error. In the regression analysis a linear relationship was established between thicknesses vs stresses and displacements. It was highlighted that the R-squared values for the ERS are superior to that of the RTS. This can be due to the uniform contact of rail (continuous support) with the concrete slab of ERS, which is not the case in the RTS (discrete contact at each rail/sleeper connection). This also signifies that stress and displacement do not vary abruptly with the change in thickness in ERS.

Work is underway by the authors to examine the effects of other structural layers and their engineering properties, loading forces system at bends, dynamic loading, etc. of these two HSR systems and another HSR track system that has the rail laid directly on a continuous resilient pad that overlays the concrete slab and extends along the full length of the rail making it a continuously supported rail rather than a discretely supported one.

ACKNOWLEDGEMENTS

The 3D model of the Embedded Rail System (ERS) is based on the information and valuable inputs provided by Charles Penny of the Embedded Rail Technology Ltd. (Penny, 2019). All values are approximated as information regarding dimensions is classified.

REFERENCES

Aggestam, E., Nielsen J. C. O. and Bolmsvik R., 2018. Simulation of vertical dynamic vehicle–track interaction using a two-dimensional slab track model, *Vehicle System Dynamics*, 56(11), pp. 1633-1657, DOI: 10.1080/00423114.2018.1426867

Batchelor, J., 1981. Use of fibre reinforced composites in modern railway vehicles. *Materials & Design*, *2*(4), pp. 172-182.

Esveld, C., 2003. Recent developments in slab track. *European railway review*, *9*(2), pp.81-85

Esveld, C., 2010. Recent developments in high-speed track. In *1st Int. Conf. on Road and Rail Infrastructure*. Opatija, 17-18 May 2010.

Fang, M, Qiu Y , Rose JG, West R.C. Ai C., 2011. Comparative analysis on dynamic behavior of two HMA railway substructures, *Journal of Modern Transportation* 19(1) pp. 26-34

Feng, H., (2011). *3D-models of railway track for dynamic analysis*. MSc dissertation, Royal Institute of Technology (KTH), Stockholm.

Lei, X. (2016) *High Speed Railway Track Dynamics: Models, Algorithms and Applications*, Springer Verlag, Singapore.

Liu X, Zhao P, Dai F., 2011. Advances in design theories of high-speed railway ballastless tracks. *Journal of Modern Transportation*, 19(3), pp. 154-162

Markine, V. L. Man, A. P de, and Esveld, C., 2000. Optimization of an embedded rail structure using a numerical technique, *HERON*, 45(1), pp. 63-74.

Michas, G., 2012. *Slab track systems for high-speed railways*, MSc dissertation, Royal Institute of Technology (KTH), Stockholm.

Penny. C. (2019) Personal Communication.

Tayabji, S.D. and Bilow, D (2001) Concrete Slab Track State of the Practice, *Transportation Research Record* 1742 (1), pp. 87-96

Teixeira, P. F. 2003, *Contribución a la reducción de los costes de mantenimiento de las vias de altavelocidad mediante la optimización de su rigidez vertical*, PhD Thesis. UPC, Barcelona.